Published in final edited form as:
Vision Res. 2012 December 15; 75: 53–59. doi:10.1016/j.visres.2012.07.020.

The Expression of Whirlin and $Ca_v1.3\alpha_1$ is Mutually Independent in Photoreceptors

Junhuang Zou[a], **Amy Lee**[b], and **Jun Yang**[a,c,*]

[a]Department of Ophthalmology and Visual Sciences, Moran Eye Center, University of Utah, Salt Lake City, UT 84132, United States

[b]Department of Molecular Physiology and Biophysics, Otolaryngology-Head and Neck Surgery and Neurology, University of Iowa, Iowa City, IA 52242, United States

[c]Department of Neurobiology and Anatomy, University of Utah, Salt Lake City, UT 84132, United States

Abstract

Whirlin is a gene responsible for Usher syndrome type II (USH2) and congenital deafness. In photoreceptors, it organizes a protein complex through binding to proteins encoded by other USH2 genes, usherin (USH2A) and G-protein-coupled receptor 98 (GPR98). Recently, $Ca_v1.3\alpha_1$ (α_{1D}) has been discovered to interact with whirlin in vitro and these two proteins are localized to the same subcellular compartments in photoreceptors. Accordingly, it is proposed that $Ca_v1.3\alpha_1$ is in the USH2 protein complex and that the USH2 protein complex is involved in regulating Ca^{2+} in photoreceptors. To test this hypothesis, we investigated the interdependence of $Ca_v1.3\alpha_1$ and whirlin expression in photoreceptors. We found that lack of $Ca_v1.3\alpha_1$ did not change the whirlin distribution or expression level in photoreceptors. In the retina, several $Ca_v1.3\alpha_1$ splice variants were found at the RNA level. Among them, the whirlin-interacting $Ca_v1.3\alpha_1$ long variant had no change in its protein expression level in the absence of whirlin. The localization of $Ca_v1.3\alpha_1$ in photoreceptors, published previously, cannot be confirmed. Therefore, the mutual independence of whirlin and $Ca_v1.3\alpha_1$ expressions in photoreceptors suggests that $Ca_v1.3\alpha_1$ may not be a key member of the USH2 protein complex at the periciliary membrane complex.

Keywords

Usher syndrome; L-type voltage-gated Ca^{2+} channel; periciliary membrane complex; retinitis pigmentosa; whirlin

1. Introduction

Usher syndrome is the most common genetic cause of combined vision and hearing loss (Boughman & Vernon & Shaver, 1983, Hartong & Berson & Dryja, 2006, Keats & Corey, 1999). Among its three clinical types, type II (USH2) accounts for more than 50% of all Usher cases (Grondahl, 1987, Hope, et al., 1997, Rosenberg, et al., 1997, Spandau &

*Corresponding Author: Jun Yang, Ph.D., John A Moran Eye Center, University of Utah, 65 Mario Capecchi Drive, Bldg 523, Salt Lake City, Utah 84132, United States. jun.yang@hsc.utah.edu. Tel: 801-213-2591. Fax: 801-587-8314.

Rohrschneider, 2002). It manifests as retinitis pigmentosa, congenital moderate hearing loss, and absence of balance problems. The causative USH2 genes, identified so far, are Usherin (USH2A), G protein-coupled receptor 98 (GPR98), and whirlin (Ebermann, et al., 2006, Eudy, et al., 1998, Weston, et al., 2004). The proteins, encoded by these genes, are colocalized at the periciliary membrane complex (PMC) in photoreceptors (Liu, et al., 2007, Yang, et al., 2010). They are interdependent for their normal localization and expression level in these cells (van Wijk, et al., 2006, Yang et al., 2010). Therefore, USH2 proteins are believed to form a complex in vivo and defects in this complex are the primary cause underlying the USH2 pathogenesis. However, the biological function of this complex is not completely understood.

Whirlin has multiple PDZ (postsynaptic density 95; discs large; Zonula occludens-1) domains and a PR (proline-rich) region. These two functional modules are thought to be involved in protein-protein interactions. It has been shown that whirlin binds to the PDZ-binding motif (PBM) at the C-terminus of both USH2A and GPR98 (Adato, et al., 2005, van Wijk et al., 2006, Yang et al., 2010). In the absence of whirlin, USH2A and GPR98 are mislocalized and their expression levels are reduced by 70–80% (Yang et al., 2010, Zou, et al., 2011). Delivery of the whirlin cDNA back into the whirlin knockout photoreceptor can rescue these USH2A and GPR98 defects (Zou et al., 2011). Therefore, whirlin plays a role in the assembly of the USH2 protein complex. Lately, espin has been identified as a whirlin-interacting protein in both photoreceptors and hair cells (Wang, et al., 2012). In these cells, whirlin modulates the actin-regulatory function of espin. Consequently, the USH2 complex is now thought to participate in organizing the actin filament network in vivo.

Ca_v1 voltage-gated Ca^{2+} channels mediate the dihydropyridine-sensitive L-type Ca^{2+} currents in response to the depolarization of the membrane potential in electrically excitable cells (Lipscombe & Pan & Gray, 2002, Striessnig & Bolz & Koschak, 2010, Striessnig & Koschak, 2008). These channels are composed of multiple subunits, including α_1, β, and α_2-δ. Among these subunits, α_1 is the pore-forming and voltage-sensing subunit, encoded by four different genes, *$Ca_v1.1$* (α_{1S}), *$Ca_v1.2$* (α_{1C}), *$Ca_v1.3$* (α_{1D}), and *$Ca_v1.4$* (α_{1F}). A mutation in *$Ca_v1.3\alpha_1$* was found to cause congenital deafness and bradycardia in humans (Baig, et al., 2011). Its protein was reported to interact with whirlin in vitro and localized to the cellular compartments similar to those of whirlin in photoreceptors (Kersten, et al., 2010). Moreover, harmonin, a homolog of whirlin and a product of the USH1C gene, associates with $Ca_v1.3\alpha_1$ and limit the availability of $Ca_v1.3$ Ca^{2+} channels at the presynaptic membrane through a ubiquitin-dependent pathway in mouse auditory inner hair cells (Gregory, et al., 2011). In both cases, the PDZ domains of whirlin and harmonin bind to the PBM at the distal $Ca_v1.3\alpha_1$ C-terminus. Based on these findings, it has been proposed that whirlin contributes to the targeting/anchoring of the $Ca_v1.3$ channel through interacting with its α_1 subunit and that $Ca_v1.3\alpha_1$ is a novel component of the USH2 complex at the PMC in photoreceptors (Kersten et al., 2010). Here, we tested these hypotheses by investigating the relationship between $Ca_v1.3\alpha_1$ and whirlin expression using whirlin and *$Ca_v1.3\alpha_1$* mutant mice. Our results demonstrate that the expression of $Ca_v1.3\alpha_1$ and whirlin is mutually independent in the photoreceptor.

2. Methods

2.1 Antibodies and animals

The polyclonal rabbit whirlin, rabbit $Ca_v1.3\alpha_1$, and chicken rootletin antibodies were described previously (Gregory et al., 2011, Yang, et al., 2002, Yang et al., 2010, Zou et al., 2011). The commercial $Ca_v1.3\alpha_1$ antibodies were purchased from Sigma-Aldrich (HPA020215, St. Louis, MO), Alomone Labs, Ltd. (ACC-005, Jerusalem, Israel), Millipore (AB5158, Temecula, CA), and Neuromab (clones L48A/9 and N38/8, Davis, CA). The

rabbit polyclonal actin (A2066) and mouse monoclonal acetylated α-tubulin (T6793) antibodies were from Sigma-Aldrich (St. Louis, MO). The Alexa fluorochrome-conjugated and the horseradish peroxidase-conjugated secondary antibodies were obtained from Invitrogen (Carlsbad, CA) and Jackson Immunoresearch laboratories, Inc. (West Grove, PA), respectively. An aliquot of the rabbit whirlin antibody was biotin-labeled according to the manufacturer's instructions (FluoReporter® mini-biotin-XX protein labeling kit, Invitrogen, Carlsbad, CA).

Whirlin (*Whrn*^{tm1Tili}) and $Ca_v1.3\alpha_1$ (*Cacna1d*^{tm1Jst}) mutant mice were described previously (Platzer, et al., 2000, Yang et al., 2010). Both have a mixed genetic background of C57BL6 and 129Sv. Their genotypes were confirmed by PCR (Table 1). Mice at an age between 2 and 4 months were maintained on a 12-h light, 12-h dark cycle and provided with standard laboratory chow and water ad libitum. All experiments involving animals were approved by the Institutional Animal Care and Use Committee at the University of Utah.

2.2 RNA isolation and RT-PCR

Total RNA was isolated from the mouse retina using the TRIzol Reagent (Invitrogen, Carlsbad, CA). RT (ThermoScript™ T-PCR system, Invitrogen, Carlsbad, CA) and PCR (expand long template PCR system, Roche Diagnostics, Indianapolis, IN) reactions were performed according to the manufacturers' instructions. The RT-PCR products were subjected to agarose gel electrophoresis and ethidium bromide staining. When necessary, the DNA band was cut from the agarose gel, eluted, and sent out for sequencing.

2.3 Western blotting

Two retinas from one mouse were homogenized in 100 μl of the RadioImmune Precipitation Assay (RIPA) buffer and cleared by centrifugation at 18,000 g for 10 minutes. The supernatants were either boiled for 10 minutes (whirlin signal) or incubated at room temperature for 30 minutes ($Ca_v1.3\alpha_1$ signal) with the Laemmli buffer, separated by SDS-PAGE, and transferred to a PVDF membrane. The PVDF membrane was sequentially subjected to blocking for 1 hour, primary antibody incubation overnight at 4°C and secondary antibody incubation for 1 hour. The dilution ratios were 1:1000 for our $Ca_v1.3\alpha_1$ antibody, 1:5000 for the whirlin antibody, and 1:3000 for the actin antibody. Detection of the protein bands was performed using the chemiluminescent substrate and by either exposure to X-ray films or imaging with a FluorChem Q machine (Proteinsimple, Santa Clara, CA). The intensities of unsaturated protein bands were measured using ImageJ and normalized by the actin signals in the same lanes. The normalized values were then converted to folds of wild-type using the average of the wild-types on the same blot. Student's *t*-tests were conducted to compare the values between different groups. A p value of less than 0.05 was considered to indicate a significant difference.

2.4 Immunofluorescent staining

Enucleated mouse eyes were frozen immediately on dry ice and sectioned at 10 μm using a cryostat. The retinal sections were fixed in 2% formaldehyde/PBS for 10 minutes and permeabilized by 0.2% Triton X-100/PBS for 5 minutes. Occasionally, they were fixed in 100% methanol for 30 minutes at −20°C for immunostaining of $Ca_v1.3\alpha_1$. The fixed retinal sections were then blocked in 5% goat serum/PBS for 1 hour, incubated with primary antibodies in 5% goat serum/PBS at an appropriate dilution ratio at 4°C overnight, washed several times with PBS, and then incubated with the Alexa fluorochrome-conjugated secondary antibodies in 5% goat serum/PBS for 1 hour. The dilution ratios were 1:500 for our $Ca_v1.3\alpha_1$ antibody, 1:150 for the Sigma and Alomone $Ca_v1.3\alpha_1$ antibodies, 1:1000 for the acetylated α-tubulin antibody, and 1:4000 for the whirlin and rootletin antibodies. For double staining of $Ca_v1.3\alpha_1$ and whirlin, the procedure was modified as follows. The retinal

sections were first stained with the rabbit $Ca_v1.3\alpha_1$ antibody (Sigma) and Alexa Fluor® 594 goat anti-rabbit secondary antibody as described above. Then, they were incubated with 0.45 mg/ml non-immune rabbit immunoglobulin (Jackson ImmunoResearch Laboratories, Inc., West Grove, PA) for 2 hours, washed with PBS, incubated with biotin-labeled rabbit whirlin antibody in 5% goat serum/PBS overnight at 4°C, washed with PBS, and finally incubated with Alexa Fluor®488-streptavindin in 5% goat serum/PBS for 1 hour. For other double staining in this study, primary antibodies from different species were used for double staining. Alexa Fluor® 488 and 594 secondary antibodies were followed. The stained sections were viewed and photographed on an epi-fluorescence microscope (IX51, Olympus, Tokyo, Japan) or a confocal laser scanning microscope (Model FV1000, Olympus, Tokyo, Japan).

3. Results

3.1 Whirlin distribution remains unaffected in the $Ca_v1.3\alpha_1^{-/-}$ photoreceptor

We investigated the requirement of $Ca_v1.3\alpha_1$ for whirlin distribution in photoreceptors, considering that normal whirlin expression is an indicator of the integrity of the USH2 complex based on our previous study (Yang et al., 2010). At a low magnification, the same signal pattern of whirlin, tiny dots between the inner and outer segment, was seen in wild-type and $Ca_v1.3\alpha_1^{-/-}$ retinas (Figs. 1A and 1B). Consistent with our previous reports (Yang et al., 2010, Yang, et al., 2012, Zou et al., 2011), whirlin was absent at the photoreceptor synapse. To further examine the whirlin localization at a high resolution, double immunostaining of whirlin with either acetylated α-tubulin or rootletin was performed, and the signals were captured using confocal laser scanning microscopy. Acetylated α-tubulin labels the axonemal microtubules projecting upward from the apex of the connecting cilium, while rootletin marks the rootlet originating from the basal bodies at the base of the connecting cilium and extending throughout the inner segment (Fig. 1A). In wild-type photoreceptors, whirlin signals were localized obliquely beneath the axonemal microtubule (Fig. 1C) and immediately above the rootlet (Fig. 1D). The localization of whirlin signals relative to the axonemal microtubule and the rootlet in the $Ca_v1.3\alpha_1^{-/-}$ retina was similar to that in the wild-type retina (Figs. 1C and 1D).

3.2 $Ca_v1.3\alpha_1$ is dispensable for maintaining the whirlin expression level in the retina

Western blotting analysis was carried out to compare the expression level of whirlin in the wild-type and $Ca_v1.3\alpha_1^{-/-}$ retinas. As shown previously (Yang et al., 2010, Yang et al., 2012, Zou et al., 2011), the whirlin specific band was at about 100 kDa (Fig. 2A). Other bands were non-specific, because they were present in both wild-type and whirlin deficient retinas. The whirlin bands displayed no significant difference in their signal intensity between the wild-type and $Ca_v1.3\alpha_1^{-/-}$ retinas ($p = 0.23$, Fig. 2B). Therefore, whirlin expression does not rely on the presence of $Ca_v1.3\alpha_1$ in the retina.

3.3 $Ca_v1.3\alpha_1$ long variant is expressed in the retina

$Ca_v1.3\alpha_1$ has 4 repeating domains, an EF hand domain, an IQ domain, a PCRD (proximal C-terminal regulatory domain), a CTM (C-terminal modulator) and a PBM (Fig. 3A) (Singh, et al., 2008). Each of the repeating domains has 6 transmembrane segments, S1-S6. Segments S1–S4 form a structure functioning as a voltage sensor. Segments S5–S6 are involved in forming the channel pore. $Ca_v1.3\alpha_1$ has sequence variations mainly occurring in four regions, the segment S6 of repeat I, the intracellular loop between repeats I and II, the segments S3–S4 of repeat IV, and the cytoplasmic C-terminal tail (red lines and arrows in Fig. 3A) (Hui, et al., 1991, Ihara, et al., 1995, Koschak, et al., 2001, Safa & Boulter & Hales, 2001, Shen, et al., 2006, Singh et al., 2008, Williams, et al., 1992). At the cytoplasmic C-terminal tail, the alternative use of exon 40A ($Ca_v1.3\alpha_1$40A) (Singh et al.,

2008) or the splice acceptor site in exon 39 ($Ca_v1.3\alpha_1$IQΔ) (Shen et al., 2006) (Fig. 3B) causes premature protein truncations immediately after or before the IQ domain, respectively. These truncations lead to loss of the PBM, the domain involved in the interaction with whirlin (Kersten et al., 2010). To examine the existence of the $Ca_v1.3\alpha_1$ long variant, the one with the complete C-terminal tail, in the retina, we performed RT-PCR using primers shown in Fig. 3B. We discovered a new $Ca_v1.3\alpha_1$ variant ($Ca_v1.3\alpha_1$41s), which was recently reported by two other groups (Bock, et al., 2011, Tan, et al., 2011). This variant is generated through the use of an alternative splice acceptor site in exon 41 and lacks the 5′ 154 bp of this exon. Its protein translation is frame-shifted with an addition of 14 unrelated amino acids before a stop codon (Figs. 3A and 3B). Additionally, we found the long and $Ca_v1.3\alpha_1$40A variants, but not the $Ca_v1.3\alpha_1$IQΔ variant, in the mouse retina (Fig. 3B).

3.4 Loss of whirlin does not change the protein expression level of the $Ca_v1.3\alpha_1$ long variant in the retina

Western blotting analysis using the $Ca_v1.3\alpha_1$ antibody, generated against a peptide from amino acids 1–22 of rat $Ca_v1.3\alpha_1$, detected a protein band at about 260 kDa in the wild-type retina (Fig. 4A). The size of this band was close to the predicted molecular weight of the $Ca_v1.3\alpha_1$ long variant. The specificity of this antibody was verified using the $Ca_v1.3\alpha_1^{-/-}$ mouse. To determine whether whirlin was necessary for normal expression of $Ca_v1.3\alpha_1$, we compared $Ca_v1.3\alpha_1$ western blot signals between wild-type and whirlin deficient ($Whrn^{tm1Till}$) retinas. We took the retinal samples from both sets of mice at the same time of day, because expression of $Ca_v1.3\alpha_1$ may change during the circadian cycle (Ko, et al., 2007). Statistical analyses using the Student's *t*-test showed no significant differences in the signal intensity of the $Ca_v1.3\alpha_1$ long variant between the whirlin deficient and wild-type mice ($p = 1$, Figs. 4A and 4B). Therefore, the expression level of $Ca_v1.3\alpha_1$ long variant in the retina is independent of whirlin or the integrity of the USH2 complex.

3.5 The localization of $Ca_v1.3\alpha_1$ around the PMC in photoreceptors cannot be established

In the wild-type retina, strong immunostaining signals of the Sigma $Ca_v1.3\alpha_1$ antibody were detected at the outer plexiform layer and outer limiting membrane (Fig. 5A, upper row). At a high magnification, a weak signal from the same antibody was obvious between the outer and inner segments in photoreceptors. Double immunostaining localized this weak signal immediately beneath whirlin around the PMC (Fig. 5A, middle and lower rows), below the axonemal microtubule (acetylated α-tubulin signals, data not shown), and above the rootlet (rootletin signals, data not shown). However, the same signal pattern, especially, the same weak signal between the outer and inner segments, was also observed in the $Ca_v1.3\alpha_1^{-/-}$ retina (Fig. 5A, upper and middle rows). These data indicate that the immunostaining signal around the PMC detected by the Sigma $Ca_v1.3\alpha_1$ antibody is non-specific. Furthermore, immunostaining of $Ca_v1.3\alpha_1$ using our and commercial (Alomone, Millipore, Neuromab) antibodies was conducted under two different fixation conditions, brief 2% formaldehyde incubation for 10 minutes at room temperature and methanol incubation for 30 minutes at −20°C. Compared with the signal pattern in the $Ca_v1.3\alpha_1^{-/-}$ retina, no specific signals were detected in the retina (Fig. 5B and data not shown). Therefore, the localization of $Ca_v1.3\alpha_1$ in the whirlin knockout retina was not examined.

4. Discussion

We demonstrate that $Ca_v1.3\alpha_1$ is not critical for the expression level and localization of whirlin and, thus, the integrity of the USH2 protein complex at the PMC in photoreceptors. In the retina, the $Ca_v1.3\alpha_1$ long splice variant, which has the whirlin-interacting PBM domain, is expressed, and its protein expression level does not rely on the integrity of the

USH2 protein complex. This mutual independence of $Ca_v1.3\alpha_1$ and the USH2 complex in photoreceptors suggests that the normal function of the USH2 protein complex does not directly involve the $Ca_v1.3$ channel and that defects in the $Ca_v1.3$ channel are not a main contributor in the USH2 disease mechanism.

The *$Ca_v1.3\alpha_1$* mutant mouse used in this study has a neomycin resistance cassette inserted into exon 2 of the *$Ca_v1.3\alpha_1$* gene (Platzer et al., 2000). This insertion leads to complete loss of the $Ca_v1.3\alpha_1$ protein expression and absence of L-type Ca^{2+} current in inner hair cells. Therefore, this mutant mouse is considered as a complete *$Ca_v1.3\alpha_1$* null mouse and a valid negative control for testing the specificity of various $Ca_v1.3\alpha_1$ antibodies. Using the $Ca_v1.3\alpha_1$ antibody from the same commercial source, we detected a signal pattern similar to that in the previous report (Kersten et al., 2010). However, we found the same signal pattern around the PMC in both the wild-type and *$Ca_v1.3\alpha_1$* null retinas (Fig. 5A), indicating that the signals detected by this $Ca_v1.3\alpha_1$ antibody are probably non-specific. Therefore, the localization of $Ca_v1.3\alpha_1$ around the PMC in photoreceptors requires a further examination.

The specificity of our $Ca_v1.3\alpha_1$ antibody was shown by western analysis in previous (Calin-Jageman, et al., 2007) and present work (Fig. 4A). This antibody and the antibody from Alomone were also specific for immunostaining of $Ca_v1.3\alpha_1$ in mouse inner hair cells (Brandt & Khimich & Moser, 2005, Gregory et al., 2011). However, these antibodies did not detect any specific $Ca_v1.3\alpha_1$ signals in photoreceptors, nor did other commercial antibodies we have tried. These results suggest that $Ca_v1.3\alpha_1$ may have a relatively even distribution in photoreceptors, in contrast with its highly enriched distribution at the synapse in inner hair cells. Although we presently still do not know whether $Ca_v1.3\alpha_1$ is mislocalized in the whirlin knockout photoreceptors, its normal protein expression level in the retina in the absence of whirlin suggests that its localization is probably normal.

In cochlear inner hair cells, the interaction between harmonin and $Ca_v1.3\alpha_1$ is required for the synaptic localization of harmonin as well as cell surface localization and ubiquitination of $Ca_v1.3\alpha_1$ (Gregory et al., 2011). In hippocampal neurons, the PBM of $Ca_v1.3\alpha_1$ binds to the PDZ domains of Shank, and this interaction is responsible for targeting $Ca_v1.3\alpha_1$ to the synapse (Zhang, et al., 2005). Therefore, in photoreceptors, the PBM of the $Ca_v1.3\alpha_1$ long variant may bind to a protein with PDZ domains for its normal targeting/tethering at the plasma membrane. Loss of this protein could result in mislocalization and unstable expression of $Ca_v1.3\alpha_1$. Whirlin in the USH2 complex was previously thought to be a good candidate (Kersten et al., 2010). Here we showed that $Ca_v1.3\alpha_1$ and whirlin are independent for their normal expressions. Therefore, the normal targeting/tethering of the $Ca_v1.3$ channel may require a mechanism unrelated to the USH2 complex. In the inner hair cells, $Ca_v1.3\alpha_1$ is present at the synapse at the base (Brandt & Khimich & Moser, 2005, Gregory et al., 2011), while whirlin is at the tip and the ankle-link of the stereocilia at the apex (Belyantseva, et al., 2005, Delprat, et al., 2005, Kikkawa, et al., 2005). Their localization at these two extreme opposite ends in inner hair cells suggests that they may not have a chance to directly interact. Therefore, our data, together with the findings in the inner hair cells, do not support the hypothesis that $Ca_v1.3\alpha_1$ is a key member of the USH2 protein complex in vivo.

Acknowledgments

We thank Drs. Joerg Striessnig (University of Innsbruck), Geoffrey G. Murphy (University of Michigan Medical School), and James Surmeier (Northwestern University) for providing us with the *$Ca_v1.3\alpha_1$* null mouse. This work was supported by National Institutes of Health grants EY020853 (J.Y.), EY014800 (core grant to the Department of Ophthalmology & Visual Sciences, University of Utah), EY020850 (A.L.), DC009433 (A.L.) and HL08712 (A.L.), Hope for Vision (J.Y.), Foundation Fighting Blindness (J.Y.), E. Matilda Ziegler Foundation for the Blind, Inc. (J.Y.), a startup package from the Moran Eye Center, University of Utah (J.Y.), and an unrestricted grant from

Research to Prevent Blindness, Inc., New York, NY, to the Department of Ophthalmology & Visual Sciences, University of Utah.

References

Adato A, Lefevre G, Delprat B, Michel V, Michalski N, Chardenoux S, Weil D, El-Amraoui A, Petit C. Usherin, the defective protein in Usher syndrome type IIA, is likely to be a component of interstereocilia ankle links in the inner ear sensory cells. Hum Mol Genet. 2005; 14(24):3921–3932. [PubMed: 16301217]

Baig SM, Koschak A, Lieb A, Gebhart M, Dafinger C, Nurnberg G, Ali A, Ahmad I, Sinnegger-Brauns MJ, Brandt N, Engel J, Mangoni ME, Farooq M, Khan HU, Nurnberg P, Striessnig J, Bolz HJ. Loss of Ca(v)1.3 (CACNA1D) function in a human channelopathy with bradycardia and congenital deafness. Nat Neurosci. 2011; 14(1):77–84. [PubMed: 21131953]

Belyantseva IA, Boger ET, Naz S, Frolenkov GI, Sellers JR, Ahmed ZM, Griffith AJ, Friedman TB. Myosin-XVa is required for tip localization of whirlin and differential elongation of hair-cell stereocilia. Nat Cell Biol. 2005; 7(2):148–156. [PubMed: 15654330]

Bock G, Gebhart M, Scharinger A, Jangsangthong W, Busquet P, Poggiani C, Sartori S, Mangoni ME, Sinnegger-Brauns MJ, Herzig S, Striessnig J, Koschak A. Functional properties of a newly identified C-terminal splice variant of Cav1.3 L-type Ca2+ channels. Journal of Biological Chemistry. 2011; 286(49):42736–42748. [PubMed: 21998310]

Boughman JA, Vernon M, Shaver KA. Usher syndrome: definition and estimate of prevalence from two high-risk populations. J Chronic Dis. 1983; 36(8):595–603. [PubMed: 6885960]

Brandt A, Khimich D, Moser T. Few CaV1.3 channels regulate the exocytosis of a synaptic vesicle at the hair cell ribbon synapse. Journal of Neuroscience. 2005; 25(50):11577–11585. [PubMed: 16354915]

Calin-Jageman I, Yu K, Hall RA, Mei L, Lee A. Erbin enhances voltage-dependent facilitation of Ca(v)1.3 Ca2+ channels through relief of an autoinhibitory domain in the Ca(v)1.3 alpha1 subunit. Journal of Neuroscience. 2007; 27(6):1374–1385. [PubMed: 17287512]

Delprat B, Michel V, Goodyear R, Yamasaki Y, Michalski N, El-Amraoui A, Perfettini I, Legrain P, Richardson G, Hardelin JP, Petit C. Myosin XVa and whirlin, two deafness gene products required for hair bundle growth, are located at the stereocilia tips and interact directly. Hum Mol Genet. 2005; 14(3):401–410. [PubMed: 15590698]

Ebermann I, Scholl HP, Charbel Issa P, Becirovic E, Lamprecht J, Jurklies B, Millan JM, Aller E, Mitter D, Bolz H. A novel gene for Usher syndrome type 2: mutations in the long isoform of whirlin are associated with retinitis pigmentosa and sensorineural hearing loss. Hum Genet. 2006; 121(2): 203–211. [PubMed: 17171570]

Eudy JD, Weston MD, Yao S, Hoover DM, Rehm HL, Ma-Edmonds M, Yan D, Ahmad I, Cheng JJ, Ayuso C, Cremers C, Davenport S, Moller C, Talmadge CB, Beisel KW, Tamayo M, Morton CC, Swaroop A, Kimberling WJ, Sumegi J. Mutation of a gene encoding a protein with extracellular matrix motifs in Usher syndrome type IIa. Science. 1998; 280(5370):1753–1757. [PubMed: 9624053]

Gregory FD, Bryan KE, Pangrsic T, Calin-Jageman IE, Moser T, Lee A. Harmonin inhibits presynaptic Cav1.3 Ca(2) channels in mouse inner hair cells. Nature Neuroscience. 2011; 14(9): 1109–1111.

Grondahl J. Estimation of prognosis and prevalence of retinitis pigmentosa and Usher syndrome in Norway. Clin Genet. 1987; 31(4):255–264. [PubMed: 3594933]

Hartong DT, Berson EL, Dryja TP. Retinitis pigmentosa. Lancet. 2006; 368(9549):1795–1809. [PubMed: 17113430]

Hope CI, Bundey S, Proops D, Fielder AR. Usher syndrome in the city of Birmingham--prevalence and clinical classification. Br J Ophthalmol. 1997; 81(1):46–53. [PubMed: 9135408]

Hui A, Ellinor PT, Krizanova O, Wang JJ, Diebold RJ, Schwartz A. Molecular cloning of multiple subtypes of a novel rat brain isoform of the alpha 1 subunit of the voltage-dependent calcium channel. Neuron. 1991; 7(1):35–44. [PubMed: 1648940]

Ihara Y, Yamada Y, Fujii Y, Gonoi T, Yano H, Yasuda K, Inagaki N, Seino Y, Seino S. Molecular diversity and functional characterization of voltage-dependent calcium channels (CACN4) expressed in pancreatic beta-cells. Mol Endocrinol. 1995; 9(1):121–130. [PubMed: 7760845]

Keats BJ, Corey DP. The usher syndromes. Am J Med Genet. 1999; 89(3):158–166. [PubMed: 10704190]

Kersten F, van Wijk E, van Reeuwijk J, van der Zwaag B, Maerker T, Peters T, Katsanis N, Wolfrum U, Keunen J, Roepman R, Kremer H. Association of whirlin with Cav1.3 ({alpha}1D) channels in photoreceptors, defining a novel member of the Usher protein network. Invest Ophthalmol Vis Sci. 2010; 51(5):2338–2346. [PubMed: 19959638]

Kikkawa Y, Mburu P, Morse S, Kominami R, Townsend S, Brown SD. Mutant analysis reveals whirlin as a dynamic organizer in the growing hair cell stereocilium. Hum Mol Genet. 2005; 14(3):391–400. [PubMed: 15590699]

Ko ML, Liu Y, Dryer SE, Ko GY. The expression of L-type voltage-gated calcium channels in retinal photoreceptors is under circadian control. J Neurochem. 2007; 103(2):784–792. [PubMed: 17683482]

Koschak A, Reimer D, Huber I, Grabner M, Glossmann H, Engel J, Striessnig J. alpha 1D (Cav1.3) subunits can form l-type Ca2+ channels activating at negative voltages. J Biol Chem. 2001; 276(25):22100–22106. [PubMed: 11285265]

Lipscombe D, Pan JQ, Gray AC. Functional diversity in neuronal voltage-gated calcium channels by alternative splicing of Ca(v)alpha1. Mol Neurobiol. 2002; 26(1):21–44. [PubMed: 12392054]

Liu X, Bulgakov OV, Darrow KN, Pawlyk B, Adamian M, Liberman MC, Li T. Usherin is required for maintenance of retinal photoreceptors and normal development of cochlear hair cells. Proc Natl Acad Sci U S A. 2007; 104(11):4413–4418. [PubMed: 17360538]

Platzer J, Engel J, Schrott-Fischer A, Stephan K, Bova S, Chen H, Zheng H, Striessnig J. Congenital deafness and sinoatrial node dysfunction in mice lacking class D L-type Ca2+ channels. Cell. 2000; 102(1):89–97. [PubMed: 10929716]

Rosenberg T, Haim M, Hauch AM, Parving A. The prevalence of Usher syndrome and other retinal dystrophy-hearing impairment associations. Clin Genet. 1997; 51(5):314–321. [PubMed: 9212179]

Safa P, Boulter J, Hales TG. Functional properties of Cav1.3 (alpha1D) L-type Ca2+ channel splice variants expressed by rat brain and neuroendocrine GH3 cells. J Biol Chem. 2001; 276(42):38727–38737. [PubMed: 11514547]

Shen Y, Yu D, Hiel H, Liao P, Yue DT, Fuchs PA, Soong TW. Alternative splicing of the Ca(v)1.3 channel IQ domain, a molecular switch for Ca2+-dependent inactivation within auditory hair cells. J Neurosci. 2006; 26(42):10690–10699. [PubMed: 17050708]

Singh A, Gebhart M, Fritsch R, Sinnegger-Brauns MJ, Poggiani C, Hoda JC, Engel J, Romanin C, Striessnig J, Koschak A. Modulation of voltage- and Ca2+-dependent gating of CaV1.3 L-type calcium channels by alternative splicing of a C-terminal regulatory domain. J Biol Chem. 2008; 283(30):20733–20744. [PubMed: 18482979]

Spandau UH, Rohrschneider K. Prevalence and geographical distribution of Usher syndrome in Germany. Graefes Arch Clin Exp Ophthalmol. 2002; 240(6):495–498. [PubMed: 12107518]

Striessnig J, Bolz HJ, Koschak A. Channelopathies in Cav1.1, Cav1.3, and Cav1.4 voltage-gated L-type Ca2+ channels. Pflugers Arch. 2010; 460(2):361–374. [PubMed: 20213496]

Striessnig J, Koschak A. Exploring the function and pharmacotherapeutic potential of voltage-gated Ca2+ channels with gene knockout models. Channels (Austin). 2008; 2(4):233–251. [PubMed: 18719397]

Tan BZ, Jiang F, Tan MY, Yu D, Huang H, Shen Y, Soong TW. Functional characterization of alternative splicing in the C terminus of L-type CaV1.3 channels. Journal of Biological Chemistry. 2011; 286(49):42725–42735. [PubMed: 21998309]

van Wijk E, van der Zwaag B, Peters T, Zimmermann U, Te Brinke H, Kersten FF, Marker T, Aller E, Hoefsloot LH, Cremers CW, Cremers FP, Wolfrum U, Knipper M, Roepman R, Kremer H. The DFNB31 gene product whirlin connects to the Usher protein network in the cochlea and retina by direct association with USH2A and VLGR1. Hum Mol Genet. 2006; 15(5):751–765. [PubMed: 16434480]

Wang L, Zou J, Shen Z, Song E, Yang J. Whirlin interacts with espin and modulates its actin-regulatory function: an insight into the mechanism of Usher syndrome type II. Human Molecular Genetics. 2012; 21(3):692–710. [PubMed: 22048959]

Weston MD, Luijendijk MW, Humphrey KD, Moller C, Kimberling WJ. Mutations in the VLGR1 gene implicate G-protein signaling in the pathogenesis of Usher syndrome type II. Am J Hum Genet. 2004; 74(2):357–366. [PubMed: 14740321]

Williams ME, Feldman DH, McCue AF, Brenner R, Velicelebi G, Ellis SB, Harpold MM. Structure and functional expression of alpha 1, alpha 2, and beta subunits of a novel human neuronal calcium channel subtype. Neuron. 1992; 8(1):71–84. [PubMed: 1309651]

Yang J, Liu X, Yue G, Adamian M, Bulgakov O, Li T. Rootletin, a novel coiled-coil protein, is a structural component of the ciliary rootlet. J Cell Biol. 2002; 159(3):431–440. [PubMed: 12427867]

Yang J, Liu X, Zhao Y, Adamian M, Pawlyk B, Sun X, McMillan DR, Liberman MC, Li T. Ablation of whirlin long isoform disrupts the USH2 protein complex and causes vision and hearing loss. PLoS Genet. 2010; 6(5):e1000955. [PubMed: 20502675]

Yang J, Wang L, Song H, Sokolov M. Current understanding of usher syndrome type II. Frontiers in Bioscience. 2012; 17:1165–1183. [PubMed: 22201796]

Zhang H, Maximov A, Fu Y, Xu F, Tang TS, Tkatch T, Surmeier DJ, Bezprozvanny I. Association of CaV1.3 L-type calcium channels with Shank. J Neurosci. 2005; 25(5):1037–1049. [PubMed: 15689539]

Zou J, Luo L, Shen Z, Chiodo VA, Ambati BK, Hauswirth WW, Yang J. Whirlin Replacement Restores the Formation of the USH2 Protein Complex in Whirlin Knockout Photoreceptors. Invest Ophthalmol Vis Sci. 2011; 52(5):2343–2351. [PubMed: 21212183]

Highlights

- Interdependence between whirlin and $Ca_v1.3\alpha1$ was studied in photoreceptors.
- $Ca_v1.3\alpha1$ is dispensable for the integrity of the USH2 complex.
- The long $Ca_v1.3\alpha1$ isoform with a PBM is expressed in the retina.
- The expression of the long $Ca_v1.3\alpha1$ isoform is normal in the absence of whirlin.

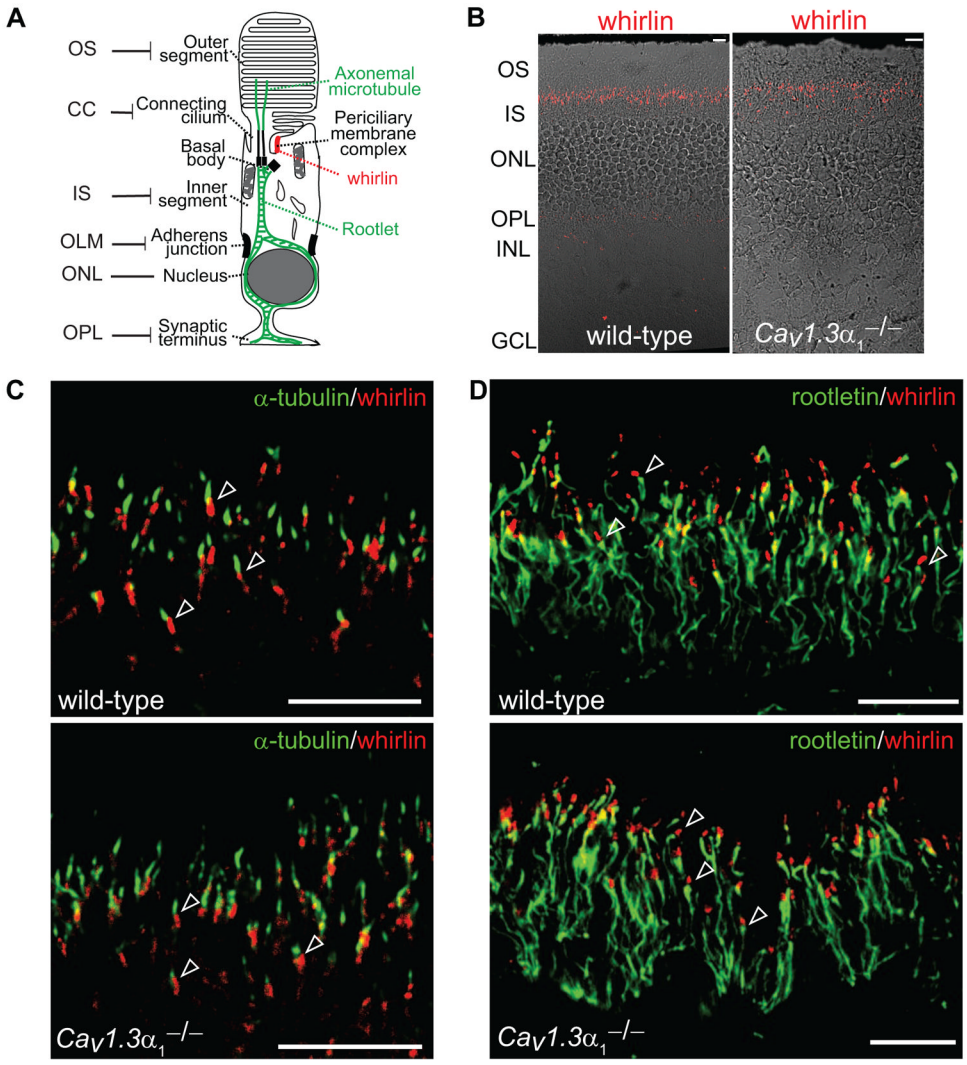

Fig 1. Whirlin distribution remains unchanged in the $Ca_v1.3\alpha_1$ null photoreceptor

(A) A schematic diagram of the various structures in a rod photoreceptor. The structure in red is the periciliary membrane complex (PMC), where the three USH2 proteins are located. The structures in green are the axonemal microtubule and rootlet, labeled by the acetylated α-tubulin and rootletin antibodies, respectively, in this study. OS, outer segment; CC, connecting cilium; IS, inner segment; OLM, outer limiting membrane; ONL, outer nuclear layer; OPL, outer plexiform layer. (B) Low magnification images showing whirlin distribution (red) in the wild-type and $Ca_v1.3\alpha_1$ null ($Ca_v1.3\alpha_1^{-/-}$) retinas. The fluorescent images are superimposed with the corresponding differential interference contrast images. (C) Confocal laser scanning images showing that whirlin (red) at the PMC is slightly obliquely beneath the axonemal microtubule (acetylated α-tubulin, green) in both the wild-type and $Ca_v1.3\alpha_1$ null retinas (arrows). (D) Confocal laser scanning images showing the same distribution of whirlin (red) related to the rootlet (rootletin, green) in the wild-type and $Ca_v1.3\alpha_1$ null retinas. Whirlin is immediately above rootletin (arrows). Scale bars, 10 μm.

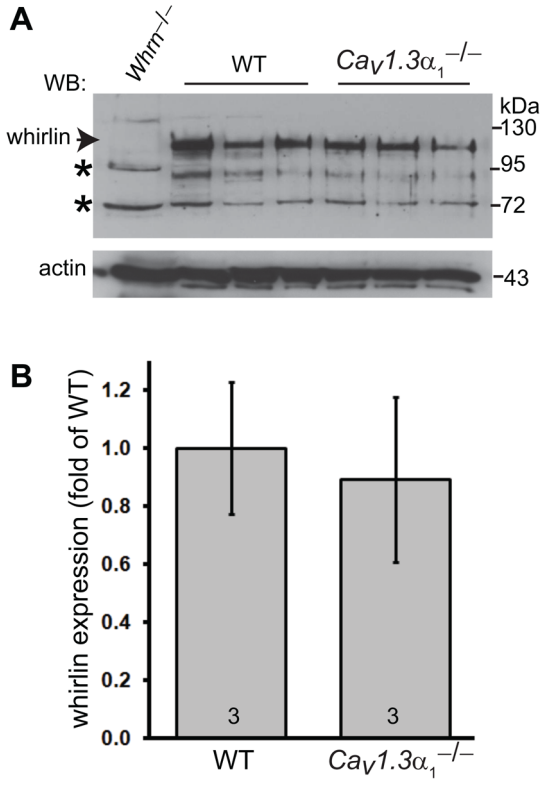

Fig 2. Whirlin expression level is not affected in the $Ca_V1.3\alpha_1$ null retina

(A) Western blotting analysis shows no obvious difference in the whirlin expression level between the wild-type (WT) and $Ca_V1.3\alpha_1$ null (*$Ca_V1.3\alpha_1^{-/-}$*) retinas. The arrow indicates the whirlin-specific band, and the asterisks indicate non-specific signals. The whirlin knockout retina (*$Whrn^{-/-}$*) was used as a negative control. Actin signals on the same blot were shown in the bottom. The samples in different lanes are from different mice. (B) Quantitative analysis of whirlin signals on the western blot. The non-specific band at about 72 kDa on the whirlin blot was used as a sample loading control for each lane. The mean of the wild-type whirlin signals normalized by the sample loading control was defined as 1. The numbers at the bottom of each bar are numbers of animals examined. Error bars, the standard error of the mean.

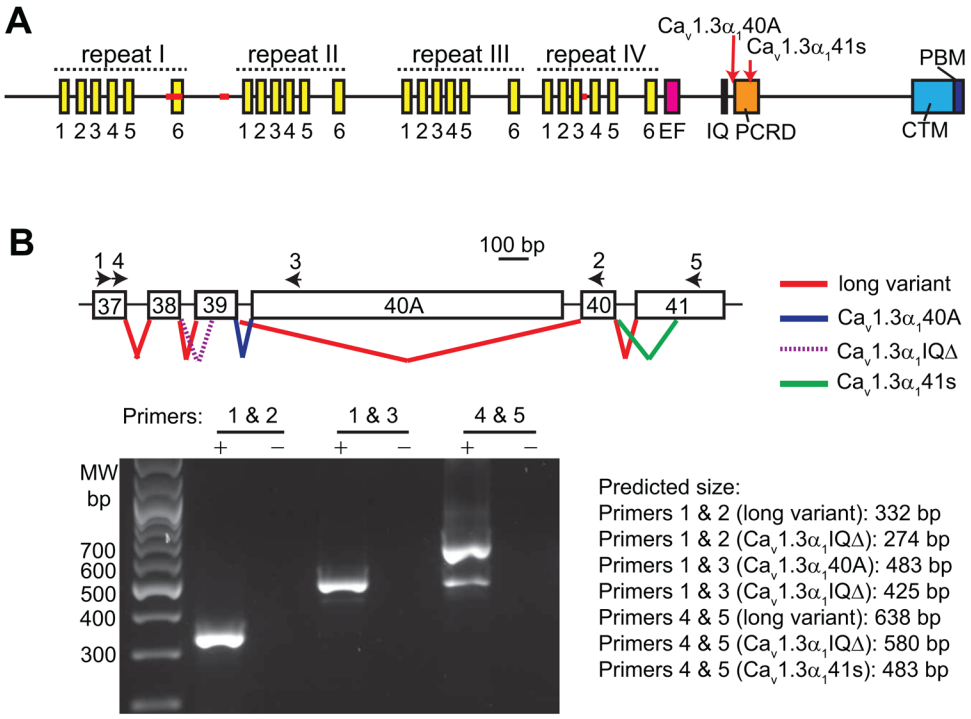

Fig 3. $Ca_v1.3\alpha_1$ domain structure and its alternative splicings in the retina

(A) A schematic diagram of the $Ca_v1.3\alpha_1$ domain structure. Red lines and arrows designate the common alternative splicing regions. $Ca_v1.3\alpha_1$40A and $Ca_v1.3\alpha_1$41s are two variants in the retina, derived from alternative splicings at the $Ca_v1.3\alpha_1$ C-terminal cytoplasmic region (see (B)). Each yellow bar represents a transmembrane segment. IQ, IQ calmodulin-binding motif; PCRD, proximal C-terminal regulatory domain; CTM, C-terminal modulator; PBM, PDZ-binding motif. (B) Alternative splicings at the C-terminal $Ca_v1.3\alpha_1$ in the mouse retina. Top, a schematic diagram of the currently known splicing events (colored lines) between exons 37 and 41. Exons are numbered according the $Ca_v1.3\alpha_1$ sequence, NM_001083616. Arrows indicate the position of primers used in RT-PCR. Bottom, image of the RT-PCR products on an agarose gel. +, PCR using the RT reaction as the template; -, PCR using water as the template, a negative control. The predicted size of the RT-PCR products from various $Ca_v1.3\alpha_1$ splice variants and primer combinations is listed on the right of the image.

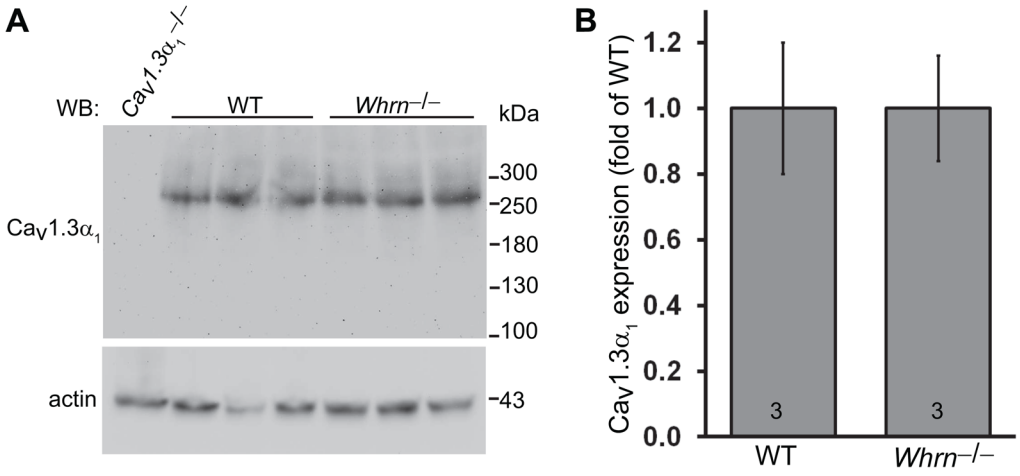

Fig 4. Protein expression level of the $Ca_v1.3\alpha_1$ long variant is normal in the whirlin deficient retina

(A) Western blotting using our $Ca_v1.3\alpha_1$ antibody displays no difference in the $Ca_v1.3\alpha_1$ long variant expression between the wild-type and whirlin deficient (*Whrn*$^{-/-}$) retinas. The $Ca_v1.3\alpha_1$ null retina (*Ca*$_v$*1.3α*$_1^{-/-}$) was used as a negative control. Actin signals on the same blot are shown in the bottom and used as a sample loading control. (B) Quantitative analysis of $Ca_v1.3\alpha_1$ signals from the wild-type and whirlin deficient retinas on the western blot using our $Ca_v1.3\alpha_1$ antibody. The mean of the normalized $Ca_v1.3\alpha_1$ signals in the wild-type retina was defined as 1. The numbers at the bottom of each bar are the numbers of animals examined in each group. Error bars, the standard error of the mean.

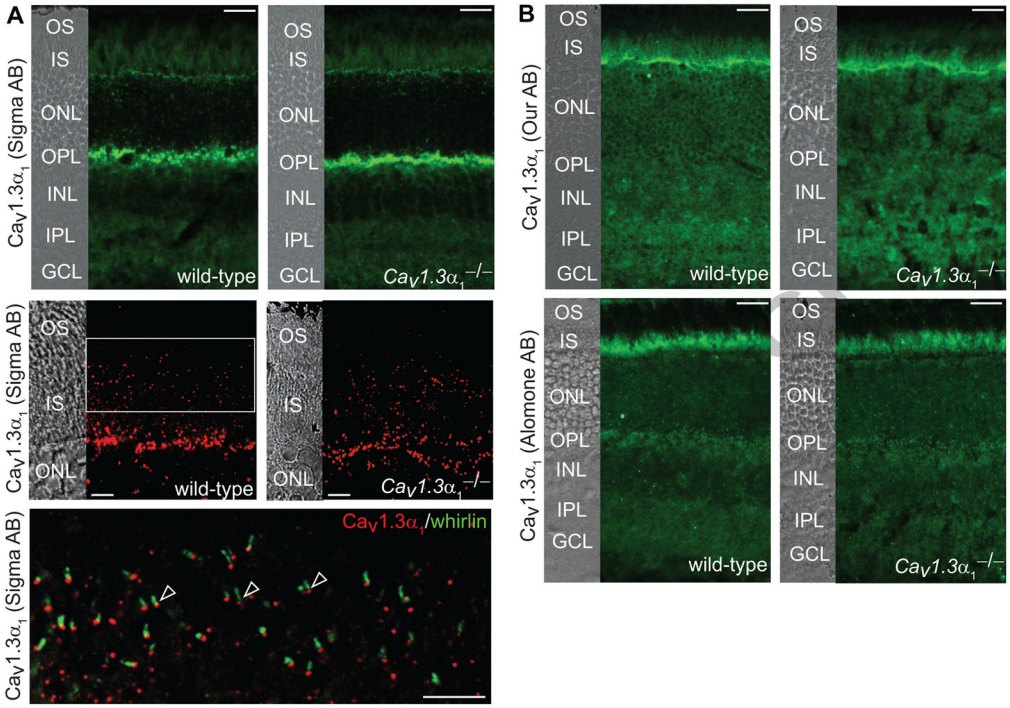

Fig 5. The localization of $Ca_V1.3\alpha_1$ around the PMC in photoreceptors cannot be established

(A) The signal pattern in the retina detected by the Sigma $Ca_V1.3\alpha_1$ antibody. *Upper row*, there is no difference in the signal pattern between wild-type and $Ca_V1.3\alpha_1$ null ($Ca_V1.3\alpha_1^{-/-}$) retinas. Non-specific signals are present in various layers of the retina except the outer segment (OS) and the outer nuclear layer (ONL). The strongest non-specific signal was detected at the outer plexiform layer (OPL). *Middle row*, weak signals were found between the OS and inner segments (IS) in both wild-type and $Ca_V1.3\alpha_1$ null retinas, indicating they are non-specific signals. *Lower row*, a zoom-in view from the region highlighted by a frame in the middle row wild-type image. The weak non-specific signals between the OS and IS detected by the Sigma $Ca_V1.3\alpha_1$ antibody (red) is immediately beneath whirlin (green). The images from the middle and lower rows were captured by confocal laser scanning microscopy. (B) The signal patterns of the retina detected by our and the Alomone $Ca_V1.3\alpha_1$ antibodies. There is no difference in these signal patterns between wild-type and $Ca_V1.3\alpha_1$ null retinas. The strongest non-specific signal of our antibody is localized to the outer limiting membrane between the IS and ONL, while the strongest non-specific signal of the Alomone $Ca_V1.3\alpha_1$ antibody is in the IS. The corresponding differential interference contrast images are on the left of most images. INL, inner nuclear layer; IPL, inner plexiform layer; GCL, ganglion cell layer. Scale bars, 20 μm (upper row in A and all images in B) and 5 μm (the middle and lower rows in A).

Table 1

Genotyping primers for whirlin and $Ca_v1.3\alpha_1^{-/-}$ deficient mice.

Whirlin	
Wild-type allele	
PDZg5r primer	CAGGGAAGTTGAGGCACACGG
PDZg1 primer	GGGTGAGTGAATGCCAGCCAG
PCR product size	894 bp
Mutant allele	
PDZg5r primer	CAGGGAAGTTGAGGCACACGG
PNT3A primer	GAGATCAGCAGCCTCTGTTCCAC
PCR product size	700 bp
$Ca_v1.3\alpha_1$	
Wild-type allele	
α1D AS primer	TACTTCCATTCCACTATACTAATGCAGGCT
α1D S primer	GCAAACTATGCAAGAGGCACCAGA
PCR product size	300 bp
Mutant allele	
α1D S primer	GCAAACTATGCAAGAGGCACCAGA
α1D NEOS primer	TTCCATTTGTCACGTCCTGCACCA
PCR product size	450 bp